Journal of Genetic Engineering and Biotechnology (2017) **15**, 31–39

HOSTED BY

ELSEVIER

Academy of Scientific Research & Technology and National Research Center, Egypt

Journal of Genetic Engineering and Biotechnology

www.elsevier.com/locate/jgeb

ORIGINAL ARTICLE

Biosynthesis, characterization and antibacterial activity of silver nanoparticles using an endophytic fungal supernatant of *Raphanus sativus*

Tej Singh [a,*], Kumari Jyoti [b,*], Amar Patnaik [c], Ajeet Singh [b], Ranchan Chauhan [d], S.S. Chandel [e]

[a] *Department of Mechanical Engineering, Manav Bharti University, Solan 173229, India*
[b] *Department of Biotechnology, G.B.P.E.C., Pauri Garhwal, 246194, India*
[c] *Department of Mechanical Engineering, M.N.I.T. Jaipur, Rajasthan 302017, India*
[d] *Faculty of Engineering and Technology, Shoolini University, Solan 173229, India*
[e] *Department of Applied Sciences, Manav Bharti University, Solan 173229, India*

Received 18 October 2016; revised 3 March 2017; accepted 8 April 2017
Available online 22 April 2017

KEYWORDS

Raphanus sativus;
Alternaria sp.;
AgNPs;
TEM;
AFM;
Antibacterial activity

Abstract In this study, biological synthesis of silver nanoparticles (AgNPs) from supernatant of endophytic fungus *Alternaria* sp. isolated from the healthy leaves of *Raphanus sativus* is studied. The synthesized AgNPs are characterized using UV-vis spectroscopy and Fourier transform-infrared spectroscopy (FTIR). The structural analysis is done by powder X-ray diffraction (XRD) method. The stability of AgNPs is studied by dynamic light scattering (DLS) method. The size and shape of AgNPs are observed by transmission electron microscopy (TEM) and atomic force microscopy (AFM) and found to be spherical with an average particles size of 4–30 nm. Further, these AgNPs have been found to be highly toxic against human pathogenic bacteria, suggesting the possibility of using AgNPs as efficient antibacterial agents.

1. Introduction

There is an increasing commercial demand for metal nanoparticles due to their potential applicability in various areas such as electronics, catalysis, energy, textile and medicine [31,41,17]. Among various metal nanoparticles, silver nanoparticles (AgNPs) in particular have been the focus of increasing interest due to their peculiar properties which can be tailored for a specific application by controlling the shape, size and morphology of the nanoparticles [49,13,15,8,4,30]. The available physical and chemical methods for metal nanoparticle synthesis resulted in low production rate, high expenditure and release of toxic chemicals [28]. Moreover, the large-scale synthesis of metal nanomaterials suffers from certain drawbacks such as stability and polydispersity, especially if the reduction is carried out in aqueous media. Thus, biological synthesis of

* Corresponding authors.
E-mail addresses: tejschauhan@gmail.com (T. Singh), jyoti490sharma@gmail.com (K. Jyoti).

Peer review under responsibility of National Research Center, Egypt.

http://dx.doi.org/10.1016/j.jgeb.2017.04.005

AgNPs provides a promising alternative offering advantages such as environment friendly, easily scaled up for large-scale synthesis and there is no need to use high pressure, temperature and toxic chemicals [28]. Biological methods based on microbes such as fungi, bacteria and viruses are able to absorb and accumulate metals and can be used in the reduction and control of nanostructural topography of metal ions and thus used for the synthesis of nanoparticles [35]. Endophytic fungus are more ideal for the synthesis of nanoparticles as the fungi could form large biomass which can withstand agitation and flow pressure and other conditions in bioreactors or other chambers and be compared to bacteria and plant materials [20]. These are fastidious to grow, secrete large amount of enzymes and are easily handled in downstream processing and thus easy for fabrication of AgNPs and can be directly used in various applications. In pharmaceutical industry, AgNPs are the most promising as they show good antibacterial activity against an array of pathogens due to their large surface area to volume ratio. One such size-dependent property has led to the development of dressing materials incorporated with nano-sized silver to enhance the wound healing property of the dressing materials [50]. The biosynthesized AgNPs have been applied widely to prevent biomedical devices associated infections, food preservation, water purification, clothing, cosmetics and other numerous pharmaceutical products [14,23,47,6].

Endophytes are microorganisms that reside inside living internal tissue of plants without inflicting any immediate, overt negative effects to the host plants [44]. Endophytes have mutualistic relationship to their host, often protecting plants against pathogens and in some cases they can act as opportunistic pathogens [43]. Drug resistance in human pathogens is a big challenge in fields such as pharmaceutical and biomedicine. One such prime focus of the pharmaceutical sector is to develop potent antibacterial drugs to combat drug-resistant pathogens which are growing at alarming pace with limited choice of available antibiotics [38]. At present, various conventional strategies using standard antibacterial agents have been used for the treatment and prevention of pathogenic bacteria. But, some of the bacterial strains have acquired resistance against available antibiotic therapies and pose the greatest risk of infection which necessitates the search for alternative drug or natural antibacterial. Therefore, modification or development in antimicrobial compounds to improve bactericidal potential is a priority area of research in the modern era. Thus, endophyte studies have been important to discover substances which will be utilized in a wide variety of disease causing agents [44].

Endophytes may produce a plethora of substances having use in modern medicine, agriculture, antimycotics, immunosuppressant and anticancer compounds [10]. To date, the endophytes have been most extensively studied for their ability to produce antibacterial, antioxidants, anticancer, antidiabetic, antiviral and antisuppresive compounds and their use in the biosynthesis of nanoparticles was also mentioned to some extent [11,33,40,12,21]. Therefore, in the present study, endophytic fungi *Alternaria* sp. was isolated from healthy leaves of *Raphanus sativus* for biosynthesis of AgNPs. The synthesized AgNPs were characterized using UV-vis (UV-vis) spectroscopy, Fourier transform-infrared (FTIR) spectroscopy, X-ray diffraction (XRD), dynamic light scattering (DLS), transmission electron microscopy (TEM) and atomic force microscopy (AFM). The antibacterial efficacy of the synthesized AgNPs was studied against human pathogenic Gram positive (methicillin-resistant *Bacillus subtilis*, *Staphylococcus aureus*) and Gram negative (*Escherichia coli* and *Serratia marcescens*) bacteria.

2. Materials and methods

2.1. Isolation and identification of the endophytic fungus

Isolation of the endophytic fungus was carried out as described by Hallmann et al. [18], with little modifications. Fresh leaves of *R. sativus* (Radish) were collected from Sultanpur, Solan district of Himachal Pradesh, India. The collected leaves were thoroughly washed under running tap water for 5 min to remove dust and debris adhering to them. The leaf samples were surface sterilized by immersing sequentially in 70% ethanol for 3 min, 0.5% sodium hypochloride for 1 min and again 70% ethanol for 30 s and finally rinsed three times in sterile distilled water to remove sterilants and then allowed to dry under sterile condition. Then, leaf samples were cut into small pieces and inoculated on potato dextrose agar plates (PDA) and incubated at 28 °C for 5 days. Then with a sterile scalpel, the leaves of 0.5 cm size were carefully dissected and placed in Petri plates containing PDA supplemented with streptomycin sulfate (100 mg/l) to suppress the bacterial growth. The plates were sealed using parafilm and incubated at 25 ± 1 °C until

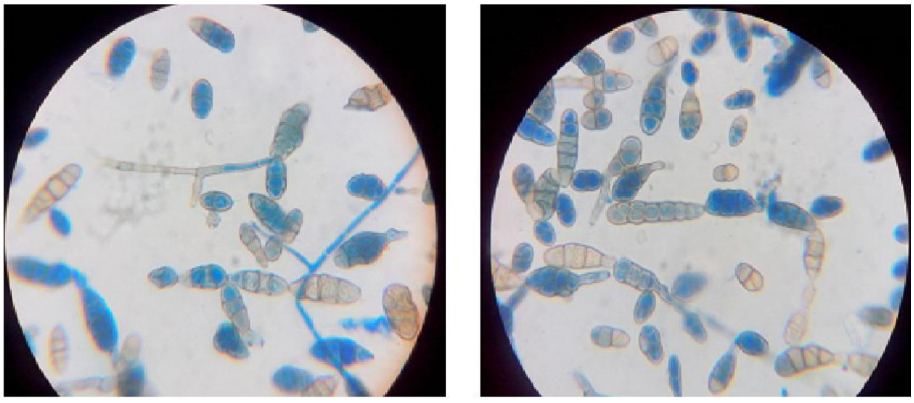

Figure 1 Microscopic view of endophytic fungus *Alternaria* sp.

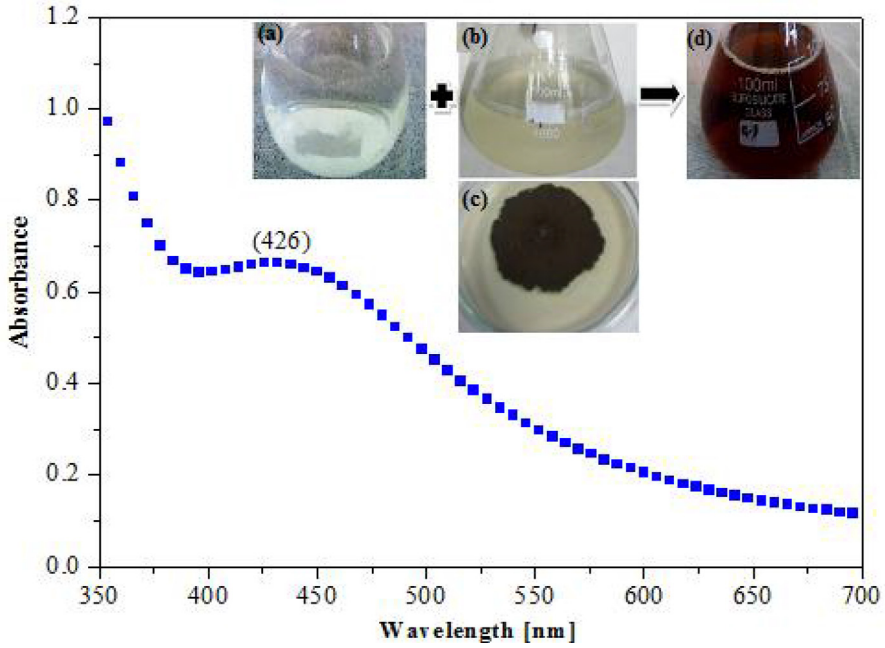

Figure 2 Optical spectra of AgNPs. Insert: (a) 1 mM $AgNO_3$, (b) Endophytic fungal culture supernatant, (c) Endophytic fungus *Alternaria* sp. and (d) Color change of $AgNO_3$ with the addition of *Alternaria* sp. fungal supernatant from white to dark brown.

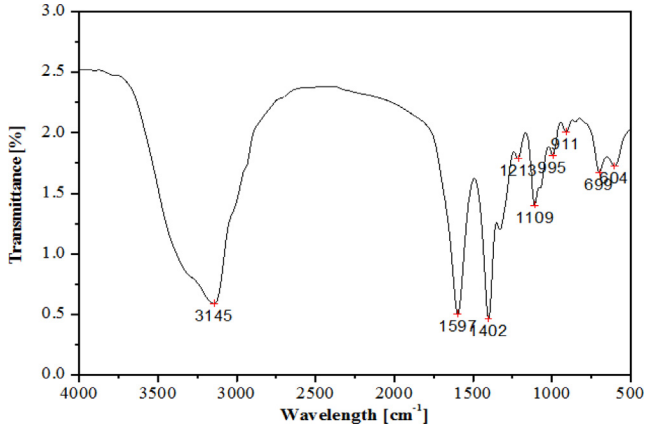

Figure 3 FTIR spectra of AgNPs.

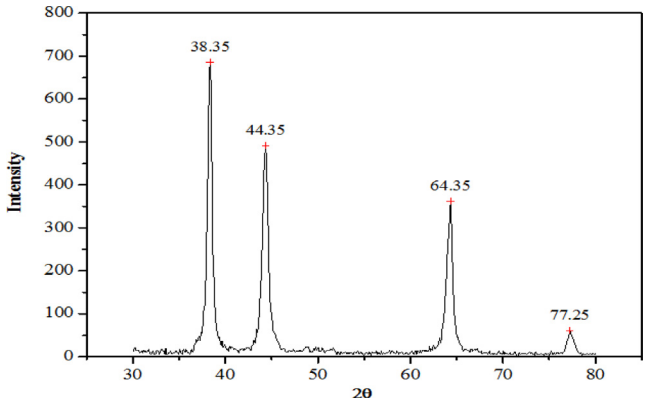

Figure 4 XRD pattern of AgNPs.

endophytic fungi emerged. As and when the hyphal tips emerged out from plant segments they were isolated, subcultured and brought to pure culture by serial subculturing. Lactophenol cotton blue staining method was used for staining the fungal culture and visualized under microscope (Quasmo, India) [39]. Identification of fungal endophytes was carried out based on morphotaxonomic characteristics (i.e. the color, shape and growth of cultured colonies), microscopic characteristics (i.e. the structure of hyphae, conidia and conidiophores) and using standard identification manuals [36]. Isolated endophytic fungus (Fig. 1) is identified as *Alternaria* sp.

2.2. Fungal fermentation of Alternaria sp.

A loopful of fungus *Alternaria* sp. was inoculated in two 500 ml Erlenmeyer conical flasks containing 200 ml of fermentation medium (Potato dextrose broth), and then incubated at 28 °C on a rotary shaker for 72 h. The biomass was harvested after 72 h of growth by filtration through muslin cloth followed by extensive washing with distilled water to remove any medium component. After that, the washed fungal biomass was filtered and weighed. For hot percolation treatment, 10 g of the fungal biomass was boiled with 100 ml of double-distilled water for 2 h and then kept undisturbed for 10 min. The resultant mixture was then filtered out using Whatman filter paper no. 1 in conical flask. This filtrate solution (namely biomass filtrate) was used for synthesis of AgNPs.

2.3. Biosynthesis of AgNPs

For AgNPs synthesis, 10 ml of mycelium free filtrate obtained from hot percolation treatment was added to 90 ml of 1 mM

aqueous silver nitrate ($AgNO_3$, Sigma-Aldrich) solution in 250 ml Erlenmeyer flask and incubated at 40 °C in a hot water bath for 20 min [46]. The color change of $AgNO_3$ from colorless to dark brown was observed by visual observation. The obtained AgNPs were purified through repeated centrifugation.

2.4. Characterization of AgNPs

Formation of AgNPs was primarily confirmed with UV-visible spectroscopy (UV-1800 Shimadzu, Japan). The absorption maximum of the sample was recorded at a resolution of 1 nm between wavelengths of 300–700 nm. The XRD patterns of the dried AgNPs were analyzed by a Panalytical X-ray ($X'Pert^3$ Powder, Netherland) diffractometer instrument operating at a voltage of 45 kV and a current of 40 mA with Cu Ka radiation. The AgNPs samples were scanned in the 2θ ranges 0–60 in the continuous scan mode and results were compared with the standard powder diffraction card No. 04-0783 of JCPDS (Joint Committee on Powder Diffraction Standards). The crystallite size of the powders was determined from X-ray line broadening using the Scherrer's equation [42] as follows:

$$D = \frac{k\lambda}{\beta \cos\theta}$$

where D is the average crystallite domain size perpendicular to the reflecting planes, k is a shape factor, λ is the X-ray wavelength (1.5418 Å), β is the full width at half maximum (FWHM), and θ is the diffraction angle. The probable biomolecules involved in the synthesis and stabilization of nanoparticles were recorded by FTIR spectrum using PerkinElmer spectrometer (Spectrum-One, U.S.A.). DLS measurements for size distribution and zeta potential were carried

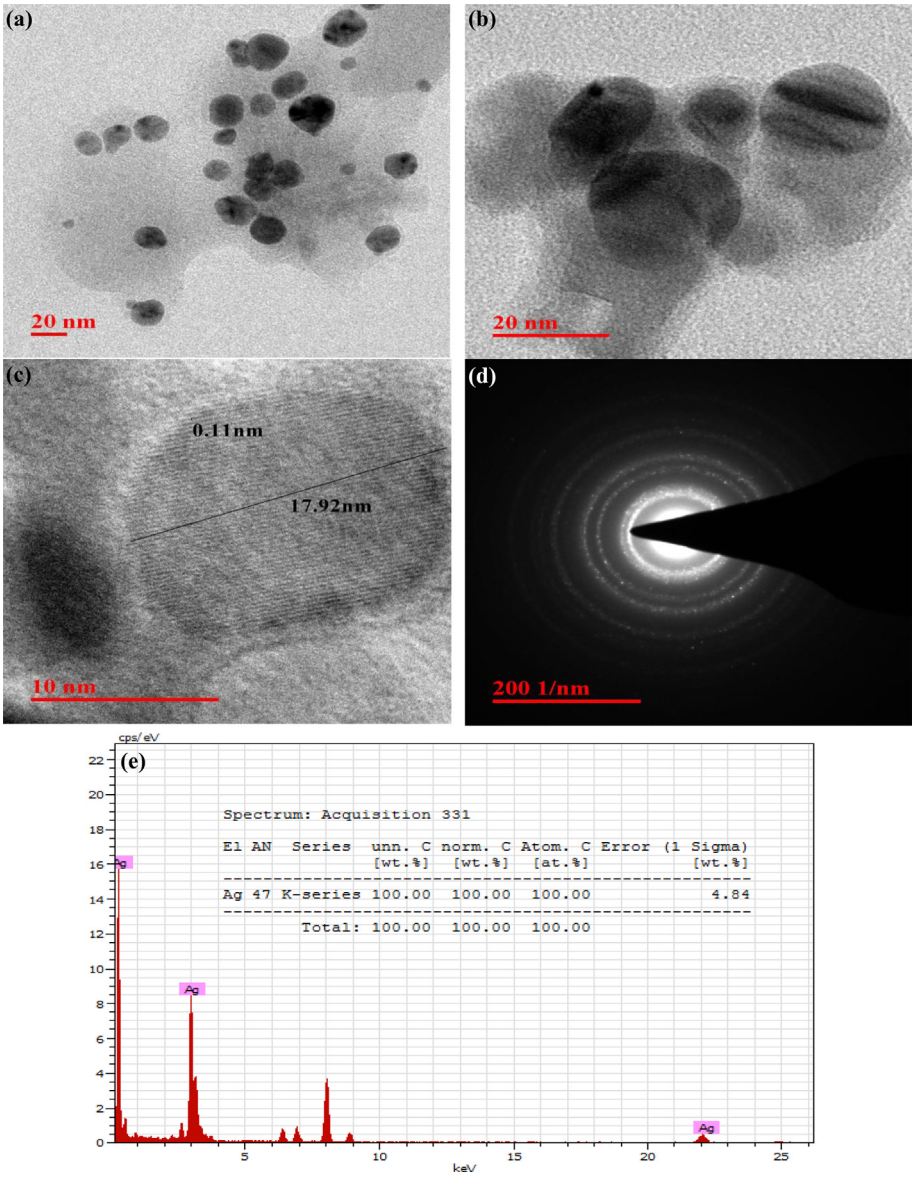

Figure 5 (a)–(c) TEM micrographs, (d) SAED pattern and (e) EDX spectrum of AgNPs.

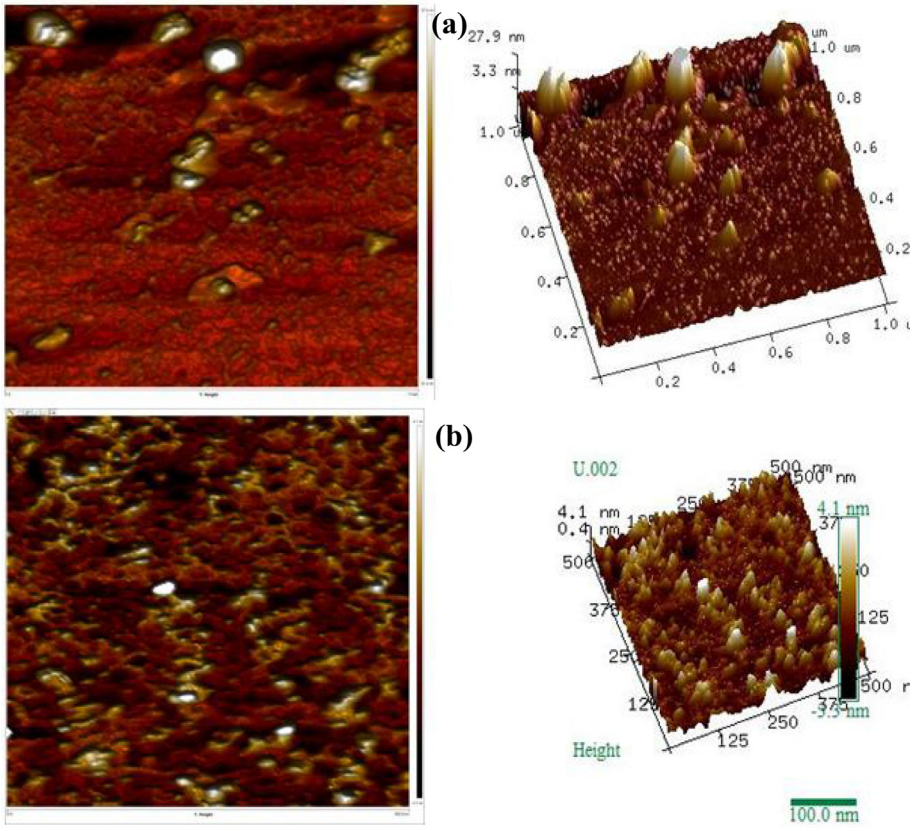

Figure 6 (a and b) AFM images of AgNPs.

out using Zetasizer Nano S90 (Malvern Instruments Ltd., U. K.). Morphology, size, selected area electron diffraction (SAED) pattern and elemental analysis were examined using TecnaiG20, Super twin, double tilt, 200 kV TEM instrument (FEI, Netherland) and AFM in non-contact mode. For TEM analysis, samples in the form of thin films were prepared by drop-coating the biosynthesized AgNPs solution on a carbon coated copper grid and drying at room temperature. The interaction of the transmitted electrons resulted in an image formation which is magnified and focused on an imaging device [9]. To investigate the elemental composition of the biosynthesized AgNPs, energy dispersive X-ray (EDX) analysis was carried out using the same instrument. Samples for AFM were prepared by spin-coating the AgNPs solution into the glass slide. The slide was dried at room temperature and subjected to AFM analysis (Nanoscope8, Bruker, Germany).

2.5. Evaluation of antibacterial activity

The synthesized AgNPs were tested for their antibacterial activity against human bacterial pathogens using the standard disk diffusion method [5]. The Gram positive (methicillin-resistant *Bacillus subtilis,* MTCC 441, *Staphylococcus aureus*, MTCC 740) and Gram negative (*Escherichia coli,* MTCC 443 and *Serratia marcescens,* MTCC 97) bacterial pathogens were obtained from Microbial Type Culture Collection (MTCC), Indian Institute of Microbial Technology (IMTECH), Chandigarh. The Freshly cultured bacterial colonies of tested bacteria were used and 100 µl of inoculum was spread on Mueller-Hinton agar plates. A single colony of each test strain was grown overnight in Mueller-Hinton liquid medium on a rotary shaker at 37 °C. The inocula were prepared by diluting the overnight cultures with 0.9% NaCl to a 0.5% Mcfarland standard and applied to plates. After that, different concentrations (5, 10, 15, 20 and 25 µg/ml) of AgNPs were loaded on 6 mm size disks. Finally, inhibition zones were measured after 24 h incubation at 37 °C. The experiments were performed in triplicate and Student's *t*-test was used to evaluate statistically significant differences.

3. Results and discussion

3.1. Confirmation of AgNPs formations

UV-visible spectra were recorded to identify the AgNPs synthesis. It was observed that upon addition of the supernatant of *Alternaria* sp. into $AgNO_3$, change in color from colorless to dark brown was observed within 20 min, indicating the synthesis of AgNPs (Fig. 2). Nanostructured metallic particles such as silver and gold have free electrons abundance, and they move through conduction and valence band which is responsible for surface plasmon resonance absorption band [32]. The characteristic surface plasmon resonance peak at about 426 nm is shown in Fig. 2, which may correspond to spherical AgNPs [9,24].

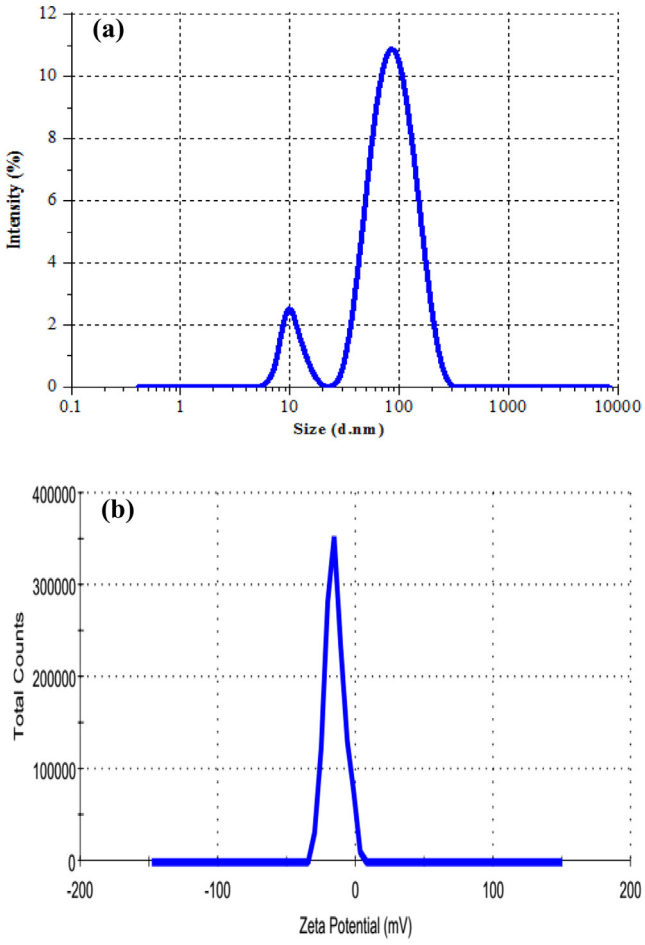

Figure 7 DLS measurements of biosynthesized AgNPs (a) Zeta sizer, (b) Zeta potential.

3.2. Study of biomolecules capping of AgNPs

FTIR spectroscopic measurements were carried out to identify the possible biomolecules responsible for capping and efficient stabilization of AgNPs synthesized by *Alternaria* sp. extract. The structure of chemical bonding formed on the synthesized AgNPs was examined by FTIR, to elucidate the nature of interaction between endophytic fungal extract and AgNPs. The FTIR spectrum of AgNPs is shown in Fig. 3, which manifests absorption peaks located at the region about 4000 cm^{-1} and 500 cm^{-1}.

FTIR spectrum shows absorption bands at 3145 cm^{-1}, 1597 cm^{-1}, 1402 cm^{-1}, 1109 cm^{-1} and 1213 cm^{-1} 995 cm^{-1} and 911 cm^{-1} 699 cm^{-1} and 504 cm^{-1} indicating the presence of capping agent with the nanoparticles (Fig. 3). The broad and intense peak at 3145 cm^{-1} can be attributed to the stretching of —OH group due to inter and intra hydrogen bonding of compounds indicating the presence of phenolic compounds [7]. The band around 1597 cm^{-1} is associated with vibration of —C═C and is assigned to primary and secondary amines and amide I bonds of proteins [49,13]. The absorption band at around 1402 cm^{-1} can be attributed to methyls [2]. The band around 1109 cm^{-1} and 1213 cm^{-1} can be attributed to C—N stretching vibration of amines indicating the presence of amino acid [49]. The band around 995 cm^{-1} and 911 cm^{-1} can be ascribed to C—H stretching vibration indicating the presence of alkene groups [45]. The band at 699 cm^{-1} and 504 cm^{-1} can be attributed to alkyl halides stretching [25].

3.3. Structural analysis

The crystalline nature of the AgNPs was clarified with XRD analysis (Fig. 4). The peaks at 2θ = 38.35, 44.35, 64.35 and 77.25 corresponding to (1 1 1), (2 0 0), (2 2 0) and (3 1 1) Bragg's reflection planes are observed. The XRD study indicates that the synthesized particles are face centered cubic structure of AgNPs [25]. The mean size of AgNPs was calculated using the Debye-Scherrer's equation [42] and found to be about ~25 nm.

3.4. Morphological study of AgNPs

TEM has provided insight into the morphology and the details of size of the synthesized nanoparticles (Fig. 5a–c). The synthesized AgNPs were almost spherical in shape with 10–30 nm size range.

The bright rings in SAED pattern suggest that the particles are crystalline in nature (Fig. 5d) [3]. The EDX profile (Fig. 5e) shows strong silver peaks approximately at 3 keV, which is typical for the absorption of AgNPs due to surface plasmon resonance [15]. The peak at 8 keV corresponds to copper and may be arisen due to the artifact of copper-grid on which the sample was coated [19]. Further the size and morphology of the AgNPs were determined from AFM (Fig. 6a and b). It can be seen that the AgNPs were monodispersed with average particle size of 4–28 nm which was in close agreement with XRD and TEM results.

Table 1 Inhibition zone of AgNPs, fungal supernatant and $AgNO_3$.

Pathogens	Inhibition zone (mm)						
	AgNPs					Fungal supernatant	$AgNO_3$
	5 μg/ml	10 μg/ml	15 μg/ml	20 μg/ml	25 μg/ml	5 μg/ml	5 μg/ml
Bacillus subtilis (MTCC 441)	9 ± 0.03	11 ± 0.01	13 ± 0.02	14 ± 0.04	23 ± 0.02	–	–
Staphylococcus aureus (MTCC 740)	6 ± 0.03	9 ± 0.01	10 ± 0.02	11 ± 0.03	12 ± 0.01	–	–
Escherichia coli (MTCC 443)	26 ± 0.02	28 ± 0.04	30 ± 0.03	31 ± 0.01	34 ± 0.03	–	–
Serratia marcescens (MTCC 97)	24 ± 0.04	29 ± 0.02	31 ± 0.01	33 ± 0.02	36 ± 0.03	–	–

Each value is the mean of three replicates with the standard deviation (±SD) and analyzed by Student's *t*-test. Difference with $P < 0.05$ was considered statistically significant. – indicates no zone.

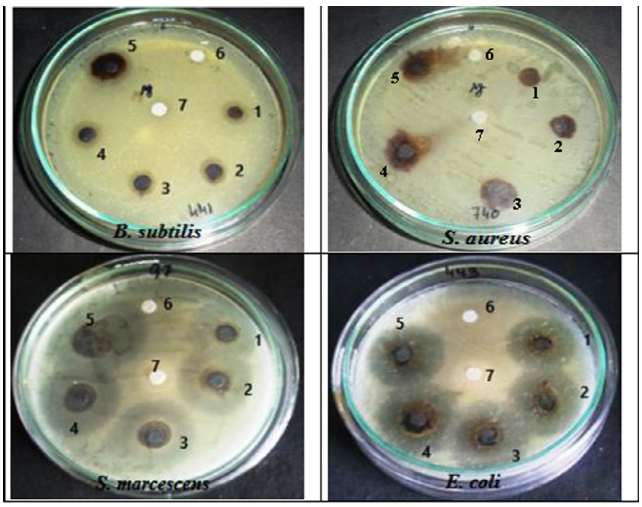

Figure 8 Images of antibacterial activity of (1) 5 μg/ml AgNP, (2) 10 μg/ml AgNP, (3) 15 μg/ml AgNP, (4) 20 μg/ml AgNP, (5) 25 μg/ml AgNP, (6) 5 μg/ml fungal supernatant and (7) 5 μg/ml $AgNO_3$.

3.5. Stability of AgNPs

The DLS measurement as shown in Fig. 7, presented the size distribution (Fig. 7a) of the AgNPs with an average size of ~80 nm and stability (Fig. 7b) for the AgNPs at −16.8 mV in zeta potential analysis. The size obtained by the DLS is different because it gives the average size of the particles. Also it could be due to the non-homogeneous dispersion of the samples. The particle size obtained from XRD, TEM, AFM and DLS is different, due to the variation in principles used for measurement [48].

3.6. Antibacterial effect of AgNPs

The antibacterial activity (as shown in Table 1 and Fig. 8) of the synthesized AgNPs against the tested human pathogens was assessed on the basis of the zone of inhibition. From Fig. 8 and Table 1, it has been observed that the biogenic AgNPs exhibited relatively high antibacterial activity against Gram-positive and Gram-negative bacteria as compared to that of controls (Fungal supernatant and $AgNO_3$). This relatively high antibacterial activity can be attributed to the size and the high surface area of the AgNPs which enabled them to reach easily the nuclear content of bacteria [27]. For the selected bacterial strains, no zone of inhibition was observed for $AgNO_3$ solution as well as extract. This symbolizes that the antibacterial potential of extract and $AgNO_3$ at their selected concentrations did not show any zone of inhibition. The irregular release of insufficient concentrations of silver ions from $AgNO_3$ may be the reason for its restricted efficacy as antimicrobial agents, which can be enhanced using AgNPs because their large surface area makes them highly reactive [1,16]. It is suggested that AgNPs may attach to the surface of the bacterial cell membrane and release silver ions which may disrupt cell membrane permeability and bacterial DNA replication [15]. In addition, nanoparticles possess extremely large surface area that provides better contact and interaction with bacterial cells [26,34]. Undoubtedly, the bactericidal activity is due to the silver cations released from AgNPs pertaining to changes in the membrane structure of bacteria, which lead to the increased membrane permeability of the bacteria and finally cell death [29].

It is apparent also from the data that increasing the concentration of the biogenic AgNPs led to a significant increase in the antibacterial activity. Kharwar et al. [21] reported the antibacterial properties of AgNPs produced by endophytic fungi, *Aspergillus clavatus* which revealed the zone of inhibition of 10 mm in case of *E. coli*. Kim et al. [22] reported similar effects on *E. coli* and *S. aureus* pathogenic strains. AgNPs synthesized by *A. flavus* were also reported to possess good antibacterial activity against *E. coli* by Ninganagouda et al. [37]. In spite of the strong antibacterial activity of biogenic AgNPs, further studies are required to investigate their bactericidal effects at a molecular level for potential widening of their applications.

4. Conclusions

In this study, an inexpensive, rapid and a single step technique for the synthesis of silver nanoparticles using endophytic fungal supernatant of *Alternaria* sp. is developed. The results of TEM and AFM have confirmed that the synthesized silver nanoparticles are mostly spherical in shape with an average size of 4–30 nm. The results of XRD, EDS and SAED confirmed the crystalline nature and elemental composition of the synthesized silver nanoparticles. These silver nanoparticles showed antibacterial activity against human pathogenic bacteria. Therefore, fungus mediated nanoparticles could be used as an excellent source against tested bacteria.

References

[1] N. Asmathunisha, K. Kathiresan, R. Anburaj, M.A. Nabeel, Synthesis of antimicrobial silver nanoparticles by callus and leaf extracts from saltmarsh plant, *Sesuvium portulacastrum* L., Colloids Surf. B 79 (2) (2010) 488–493.
[2] K. Brajesh, S. Kumari, C. Luis, D. Alexis, Sacha inchi (*Plukenetia volubilis* L.) shell biomass for synthesis of silver nanocatalyst, J. Saudi Chem. (2014), http://dx.doi.org/10.1016/j.jscs.2014.03.005.
[3] K. Brajesh, S. Kumari, C. Luis, D. Alexis, Green synthesis of silver nanoparticles using Andean blackberry fruit extract, Saudi J. Biol. Sci. (2015), http://dx.doi.org/10.1016/j.sjbs.2015.09.006.
[4] S. Chinnappan, S. Kandasamy, G. Muthusamy, S. Balakrishnan, S. Arumugam, S. Murugesan, S. Thangasamy, *Acorus calamus* rhizome extract mediated biosynthesis of silver nanoparticles and their bactericidal activity against human pathogens, J. Genet. Eng. Biotechnol. 13 (2) (2015) 93–99.
[5] M.G. Cormican, W.W. Wilke, M.S. Barrett, M.A. Pfaller, R.N. Jones, Phenotypic detection of *mec A*-positive staphylococcal blood stream isolates: high accuracy of simple disk diffusion tests, Diagn. Microbiol. Infec. Dis. 25 (1996) 107–112.
[6] R. Dastjerdi, M. Montazer, A review on the application of inorganic nano-structured materials in the modification of textiles: focus on anti-microbial properties, Colloids Surf. B 79 (2010) 5–18.
[7] A.K. Deenadayalan, V. Palanichamy, M.R. Selvaraj, Green synthesis of silver nanoparticles using *Alternanthera dentata* leaf extract at room temperature and their antimicrobial activity, Spectrochim. Acta Part A Mol. Biomol. Spectrosc. 127 (2014) 168–171.

[8] M.M. El-Sheekh, H.Y. El-Kassas, Algal production of nano-silver and gold: their antimicrobial and cytotoxic activities: a review, J. Genet. Eng. Biotechnol. 14 (2) (2016) 299–310.
[9] Z.G. Eman, Antimicrobial, antioxidant and antitumor activities of silver nanoparticles synthesized by *Allium cepa* extract: a green approach, J. Genet. Eng. Biotechnol. 15 (2017) 49–57.
[10] M. Fakruddin, Z. Hossain, H. Afroz, Prospects and applications of nanobiotechnology: a medical perspective, J. Nanotechnol. 10 (2012) 31.
[11] B.S. Fathima, R.M. Balakrishnan, Biosynthesis and optimization of silver nanoparticles by endophytic fungus *Fusarium solani*, Mater. Lett. 132 (2014) 428–431.
[12] A.K. Gade, P. Bonde, A.P. Ingle, P.D. Marcato, N. Duran, M. K. Rai, Exploitation of *Aspergillus niger* for synthesis of silver nanoparticles, J. Biobased Mater. Bioenergy 2 (3) (2008) 243–247.
[13] S.U. Ganaie, A. Tasneem, J. Anuradha, S.A. Abbasi, Biomimetic synthesis of silver nano particles using the amphibious weed ipomoea and their application in pollution control, J. King Saud Univ.-Sci. 26 (2014) 222–229.
[14] D. Gangadharan, K. Harshvardan, G. Gnanasekar, D. Dixit, K. M. Popat, P.S. Anand, Polymeric microspheres containing silver nanoparticles as a bactericidal agent for water disinfection, Water Res. 44 (18) (2010) 5481–5487.
[15] S. Ghosh, S. Patil, M. Ahire, R. Kitture, S. Kale, K. Pardesi, S. S. Cameotra, J. Belleare, D.D. Dhavale, B.A. Chopade, Synthesis of silver nanoparticles using Dioscorea bulbifera tuber extract and evaluation of its synergistic potential in combination with antimicrobial agents, Int. J. Nanomed. 7 (2012) 483–496.
[16] S. Gopal, H.G. Poosali, K. Dhanasegaran, P. Durai, D. Devadoss, R. Nagaiya, R. Balasubramanian, K. Arunagirinathan, V.S. Ganesan, Green synthesis of silver nanoparticles using *Delphinium denudatum* root extract exhibits antibacterial and mosquito larvicidal activities, Spectrochim. Acta Part A Mol. Biomol. Spectrosc. 127 (2014) 61–66.
[17] Y..El.-K. Hala, El.-A. Mohamed, Phytotoxic effects of seaweed mediated copper nanoparticles against the harmful alga: *Lyngbya majuscule*, J. Genet. Eng. Biotechnol. 15 (2017) 41–48.
[18] J. Hallmann, J.G. Berg, B. Schulz, Isolation procedures for endophytic microorganisms, Soil Biol. 9 (2007) 299–319.
[19] K. Jyoti, M. Baunthiyal, A. Singh, Characterization of silver nanoparticles synthesized using *Urtica dioica* Linn. leaves and their synergistic effects with antibiotics, J. Radiat. Res. Appl. Sci. 9 (2016) 217–227.
[20] K. Kathiresan, S. Manivannan, M.A. Nabeel, B. Dhivya, Studies on silver nanoparticles synthesized by a marine fungus, *Penicillium fellutanum* isolated from coastal mangrove sediment, Colloids Surf. B Biointerf. 71 (2009) 133–137.
[21] R.N. Kharwar, V.C. Verma, A.C. Gange, Biosynthesis of antimicrobial silver nanoparticle by endophytic fungus *Aspergillus clavatus*, Nanomedicine 5 (1) (2010) 33–40.
[22] J.S. Kim, E. Kuk, K.N. Yu, J.H. Kim, S.J. Park, H.J. Lee, S.H. Kim, Y.K. Park, Y.H. Park, C.Y. Hwang, Y.K. Kim, Y.S. Lee, D.H. Jeong, M.H. Cho, Antimicrobial effects of silver nanoparticles, Nanomedicine 3 (2007) 95–101.
[23] S. Kokura, O. Handa, T. Takagi, T. Ishikawa, Y. Naito, T. Yoshikawa, Silver nanoparticles as a safe preservative for use in cosmetics, Nanomed. Nanotechnol. Biol. Med. 6 (4) (2010) 570–574.
[24] J. Kumari, S. Ajeet, Green synthesis of nanostructured silver particles and their catalytic application in dye degradation, J. Genet. Eng. Biotechnol. 14 (2) (2016) 311–317.
[25] J. Kumari, S. Ajeet, Evaluation of antibacterial activity from phytosynthesized silver nanoparticles against medical devices infected with *Staphylococcus* spp., J. Taibah Univ. Med. Sci. 12 (1) (2017) 47–54.
[26] L. Kvitek, A. Panacek, J. Soukupova, M. Kolar, R. Vecerova, R. Prucek, M. Holecova, R. Zboril, Effect of surfactants and polymers on stability and antibacterial activity of silver nanoparticles (NPs), J. Phys. Chem. C 112 (2008) 5825–5834.
[27] C.N. Lok, C.M. Ho, R. Chen, Q.Y. He, W.Y. Yu, H. Sun, P.K. H. Tam, J.F. Chiu, C.M. Che, Proteomic analysis of the mode of antibacterial action of silver nanoparticles, J. Proteome Res. 5 (2006) 916–924.
[28] K. Mallick, M.J. Witcomb, M.S. Scurell, Polymer stabilized silver nanoparticles: a photochemical synthesis route, J. Mater. Sci. 39 (2004) 4459–4463.
[29] Y. Matsumura, K. Yoshikata, S. Kunisaki, T. Tsuchido, Mode of bactericidal action of silver zeolite and its comparison with that of silver nitrate, Appl. Environ. Microbiol. 69 (2003) 4278–4281.
[30] M.A. Mohammad, Y. Abbas, H.M. Mehdi, B. Somayeh, Effects of antimicrobial activity of silver nanoparticles on in vitro establishment of G × N15 (hybrid of almond × peach) rootstock, J. Genet. Eng. Biotechnol. 12 (2) (2014) 103–110.
[31] K.P. Mohanpuria, N.K. Rana, S.K. Yadav, Biosynthesis of nanoparticles: technological concepts and future applications, J. Nanopart. Res. 10 (2008) 507–517.
[32] P. Mulvaney, Surface plasmon spectroscopy of nanosized metal particles, Langmuir 12 (1996) 788–800.
[33] J. Mussarat, S. Dwivedi, B.R. Singh, A.A. Al-Khedhairy, A. Azam, A. Naqvi, Production of antimicrobial silver nanoparticles in water extracts of fungus *Amylomyces rouxii* strain KSU-09, Biores. Technol. 101 (22) (2010) 8772–8776.
[34] P. Muthuraman, H.K. Doo, ZnO nanoparticles augment ALT, AST, ALP and LDH expressions in C2C12 cells, Saudi J. Biol. Sci. 22 (6) (2015) 679–684.
[35] K.B. Narayanan, N. Sakthivel, Biological synthesis of metal nanoparticles by microbes, Adv. Coll. Interf. Sci. 156 (2010) 1–13.
[36] S.S. Navi, R. Bandyopadhyay, A.J. Hall, P.J.B. Cox, A Pictorial Guide for the Identification of Mold Fungi on Sorghum Grain, International Crops Research Institute for Semi Arid Tropics, India, 1999.
[37] S. Ninganagouda, V. Rathod, H. Jyoti, D. Singh, K. Prema, U. H. Manzoor, Extracellular biosynthesis of silver nanoparticles using *Aspergillus flavus* and their antimicrobial activity against gram negative MDR strains, Int. J. Pharma Bio Sci. 4 (2) (2013) 222–229.
[38] I.N. Okeke, R. Laxminarayan, Z.A. Bhutta, A.G. Duse, P. Jenkins, T.F. O'Brien, A. Pablos-Mendez, K.P. Klugman, Antimicrobial resistance in developing countries. Part I: Recent trends and current status, Lancet Infect. Dis. 5 (8) (2005) 481–493.
[39] S.C. Parija, M.R. Shivaprakash, S.R. Jayakeerthi, Evaluation of lacto-phenol cotton blue (LPCB) for detection of *Cryptosporidium*, *Cyclospora* and *Isospora* in the wet mount preparation of stool, Acta Trop. 85 (2003) 349–354.
[40] F. Rahman, S. Deshmukh, A. Ingle, A. Gade, M. Rai, Silver nanoparticles: novel antimicrobial agent synthesized from an endophytic fungus *Pestalotia* sp. isolated from leaves of Syzygium cumini, Nano Biomed. Eng. 3 (3) (2011) 174–178.
[41] S. Rajeshkumar, Anticancer activity of eco-friendly gold nanoparticles against lung and liver cancer cells, J. Genet. Eng. Biotechnol. 14 (1) (2016) 195–202.
[42] R.B. Rajkiran, B.N. Veera, R.K. Pratap, Green synthesis and characterization of *Carica papaya* leaf extract coated silver nanoparticles through X-ray diffraction, electron microscopy and evaluation of bactericidal properties, Saudi J. Biol. Sci. 22 (5) (2015) 637–644.
[43] N.K. Ravindra, C.V. Vijay, S. Gary, E. David, The endophytic fungal complex of *Catharanthus roseus* (L.) G. Don, Curr. Sci. 95 (2008) 228–233.

[44] G.A. Strobel, B. Daisy, Bioprospecting for microbial endophytes and their natural products, Microbiol. Mol. Biol. Rev. 67 (2003) 491–502.

[45] G.C.J. Swarnavalli, S. Dinakaran, N. Raman, R. Jegadeesh, C. Pereira, Bio inspired synthesis of monodispersed silver nano particles using *Sapindus emarginatus* pericarp extract – study of antibacterial efficacy, J. Saudi Chem. Soc. (2015), http://dx.doi.org/10.1016/j.jscs.2015.03.004.

[46] K.N. Thakkar, S.S. Mhatre, R.Y. Parikh, Biological synthesis of metallic nanoparticles, Nanomed. Nanotechnol. Biol. Med. 6 (2) (2010) 257–262.

[47] J. Tian, K.K. Wong, C.M. Ho, C.N. Lok, W.Y. Yu, C.M. Che, J.F. Chiu, P.K. Tam, Topical delivery of silver nanoparticles promotes wound healing, ChemMedChem 2 (1) (2007) 129–136.

[48] M. Veshara, B. Izel, B.N.K. Suresh, N.M. Joyce, Enhancing antidiabetic and antimicrobial performance of *Ocimum basilicum*, and *Ocimum sanctum* (L.) using silver nanoparticles, Saudi J. Biol. Sci. (2015), http://dx.doi.org/10.1016/j.sjbs.2015.06.026.

[49] V.K. Vidhu, D. Philip, Spectroscopic, microscopic and catalytic properties of silver nanoparticles synthesized using Saraca indica flower, Spectrochim. Acta Part A Mol. Biomol. Spectrosc. 117 (2014) 102–108.

[50] M. Zamani, M.P. Prabhakaran, S. Ramakrishna, Advances in drug delivery via electrospun and electrosprayed nanomaterials, Int. J. Nanomed. 8 (2013) 2997–3017.